

Supplementary Information

Two-dimensional cyano-bridged coordination polymer of $\text{Mn}(\text{H}_2\text{O})_2[\text{Ni}(\text{CN})_4]$: structural analysis and proton conductivity measurements upon dehydration and rehydration

Azhar Alowasheeir,^{a,b} Satoshi Tominaka^{a*}, Yusuke Ide^a, Yusuke Yamauchi^{c,d}
and Yoshitaka Matsushita^e

a. International Center for Materials Nanoarchitechtonics (WPI-MANA), National Institute for Materials Science (NIMS), 1-1 Namiki, Tsukuba, Ibaraki 305-0044, Japan.

b. Faculty of Science and Engineering, Waseda University, 3-4-1 Okubo, Shinjuku, Tokyo, 169-8555, Japan.

c. School of Chemical Engineering & Australian Institute for Bioengineering and Nanotechnology (AIBN), The University of Queensland, Brisbane, QLD 4072, Australia.

d. Department of Plant & Environmental New Resources, Kyung Hee University, 1732 Deogyeong-daero, Giheung-gu, Yongin-si, Gyeonggi-do 446-701, South Korea.

e. Materials Analysis Station, National Institute for Materials Science, 1-2-1 Sengen, Tsukuba, Ibaraki 305-0047, Japan.

Contents

1. Photograph of single crystal $[\text{Mn}(\text{H}_2\text{O})_2\text{Ni}(\text{CN})_4] \cdot 3\text{H}_2\text{O}$
2. Structure data obtained by single crystal and powder data for as-prepared, phase I and phase II.
3. Crystal structure of phase I obtained by SXRD.
4. Thermogravimetric analysis.
5. Distance between oxygen bond and Ni–O coordination bond on phase I and phase II.
6. Crystal structure of re-hydrated single crystal.
7. Rietveld analysis result of re-hydration sample.
8. Hydrogen bonding network and distances in phase I.
9. Image of setup for single crystal impedance analyses.
10. Single crystal AC impedance data and analyses



Fig.S1 Photograph of the $[\text{Mn}(\text{H}_2\text{O})_2\text{Ni}(\text{CN})_4]\cdot 3\text{H}_2\text{O}$ single crystal as-synthesis

Table S1 Lattice constants obtained by the SC-XRD and PXRD data

Compound	Phase I (293 K)	Phase I (113 K)	Phase I (298 K)	Phase II (298 K)	Phase I (298 K) Rehydrated phase
Formula	$\text{MnNiC}_4\text{N}_4\text{O}_6$	$\text{MnNiC}_4\text{N}_4\text{O}_6$	$\text{MnNiC}_4\text{N}_4\text{O}_{9.259}$	$\text{MnNiC}_4\text{N}_4\text{O}_{4.604}$	$\text{Mn}_{0.93}\text{NiC}_4\text{N}_4\text{O}_{9.373}$
Space group	Pnma	Pnma	Pnma	Imma	Pnma
a (Å)	12.3058(3)	12.0750(3)	12.30625(17)	14.5229(15)	12.3066(9)
b (Å)	14.1261(3)	14.0779(3)	14.12662(2)	7.2962(8)	14.1272(12)
c (Å)	7.3105(2)	7.3144(2)	7.31004(11)	9.0371(10)	7.3101(6)
(°)	90	90	90	90	90
β (°)	90	90	90	90	90
γ (°)	90	90	90	90	90
V (Å³)	1270.81(5)	1243.38(5)	1270.82(4)	957.59(2)	1270.91(2)
R1 (%) / R_{wp} (%) [*]	3.93	2.73	7.74	11.39	6.78
Method	SC-XRD	SC-XRD	Synchrotron HR-PXRD	Synchrotron HR-PXRD	Synchrotron HR- PXRD

*. Reliable indexes: R1 is for SC-XRD and R_{wp} is for synchrotron HR-XRD.

Table.S2 Selected bond lengths (Å) and angles (°) in phase I (determined by SC-XRD) at 293 K.

Ni–C1	1.8566(8)	Mn–N2	2.1950(8)
Ni–C2	1.8572(8)	N–C	1.1541(11)
Mn–O	2.2357(8)	N–C	1.1529(11)
Mn–N1	2.1979(8)	Ni–O	2.7823(18)
O4–Mn–O4	180.0	C2–N2–Mn	176.06(6)
N1–Mn–N2	90.87(4)	C1–Ni–C2	173.94(4)
N2–Mn–N1	89.13(4)	C2–Ni–C2	89.04(5)
O4–Mn–N2	87.78(4)	C1–Ni–C1	89.83(5)
O4–Mn–N1	87.38(3)	C1–Ni–C2	90.25(4)
O4–Mn–N1	92.62(3)	N1–C1–Ni	175.74(9)
C1–N1–Mn	158.59(9)	N2–C2–Ni	177.66(10)
C1–Ni–O	94.96(4)		

Table.S3 Selected bond lengths (Å) and angles (°) in phase I (determined by HR-PXRD).

Ni–C1	1.8565(9)	Mn–N2	2.1950(10)
Ni–C2	1.8573 (9)	N–C	1.307(15)
Mn–O	2.2357(9)	N–C	1.394(14)
Mn–N1	2.1980(10)	Ni–O	2.792(11)
O4–Mn–O4	180.0	C2–N2–Mn	124.5(8)
N1–Mn–N2	91.4(5)	C1–Ni–C2	177.9(6)
N1–Mn–N2	88.5(4)	C2–Ni–C2	89.1(9)
O4–Mn–N2	96.0(4)	C1–Ni–C1	86.8(7)
O4–Mn–N1	94.2(4)	C2–Ni–C1	91.9(5)
O4–Mn–N2	84.0(4)	N1–C1–Ni	109.9(9)
O4–Mn–N1	85.8(4)	N2–C2–Ni	141.5(10)
C1–N1–Mn	120.3(8)	C2–Ni–O	107.6(5)

Table S4 Selected bond lengths (\AA) and angles ($^\circ$) in phase II (determined by HR-PXRD).

Ni–C	1.774(18)	Mn–N	2.246(15)
Mn–O	2.229(14)	C–N	1.25(3)
Ni–O	3.06(2)	O–Mn–N	91.9(6)
O–Mn–O	180.0	C–N–Mn	163.9(14)
N–Mn–N	180.0	C–Ni–C	171.1(14)
N1–Mn–N2	84.9(8)	C1–Ni–C2	103.4(12)
N2–Mn–N2	95.1(8)	C2–Ni–C1	75.9(12)
O–Mn–N	88.1(6)	N–C–Ni	152.1(16)

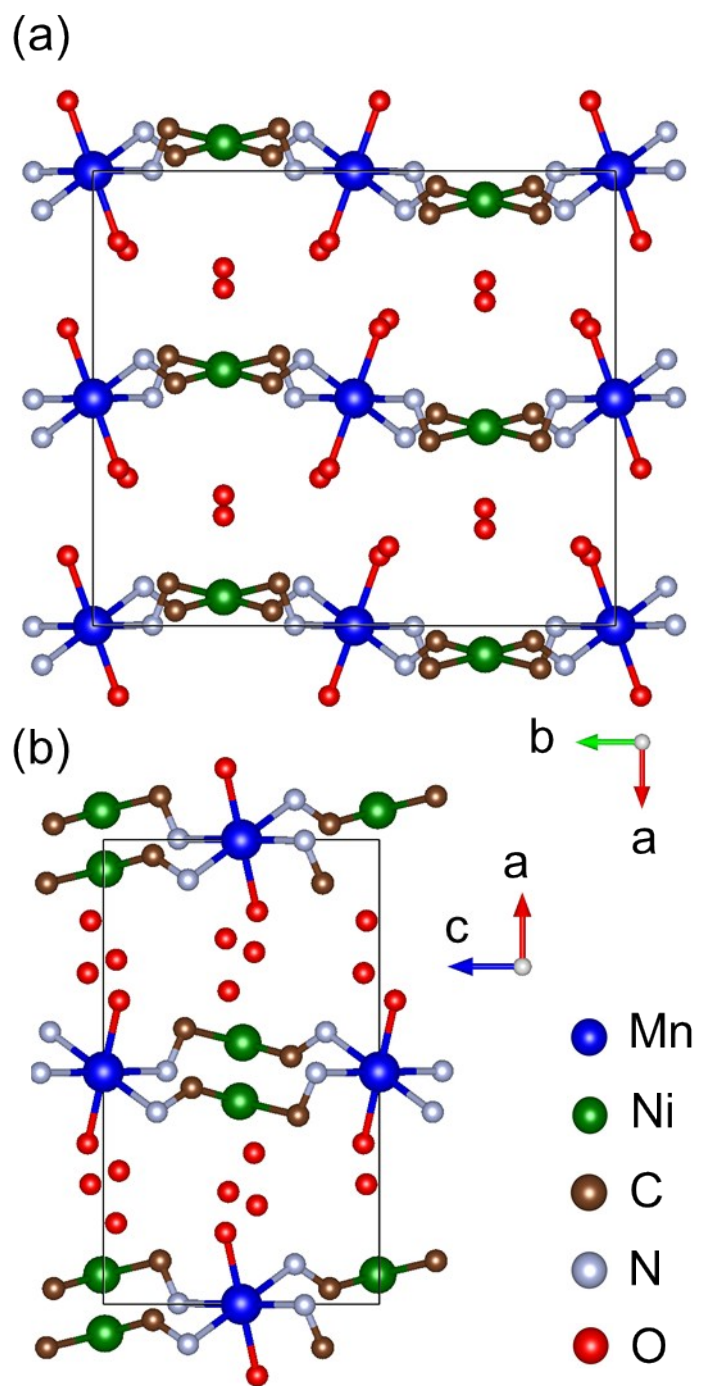


Fig.S2 Crystal structure of phase I (HR=100%) obtained by PXRD.

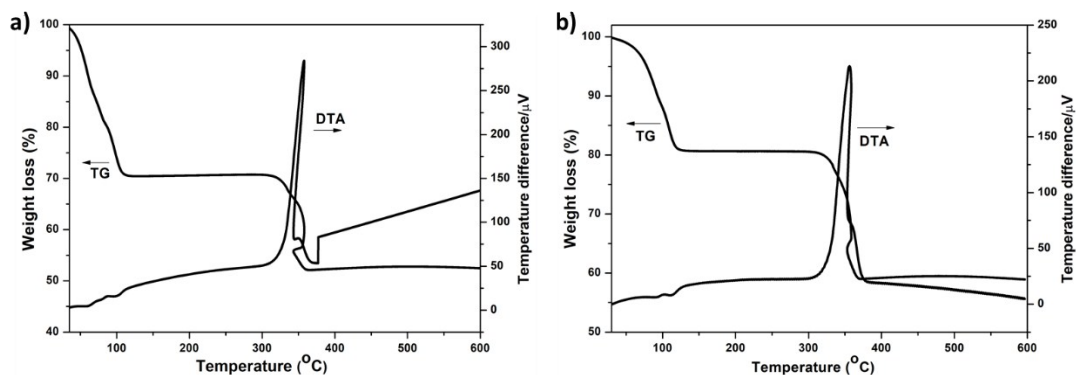
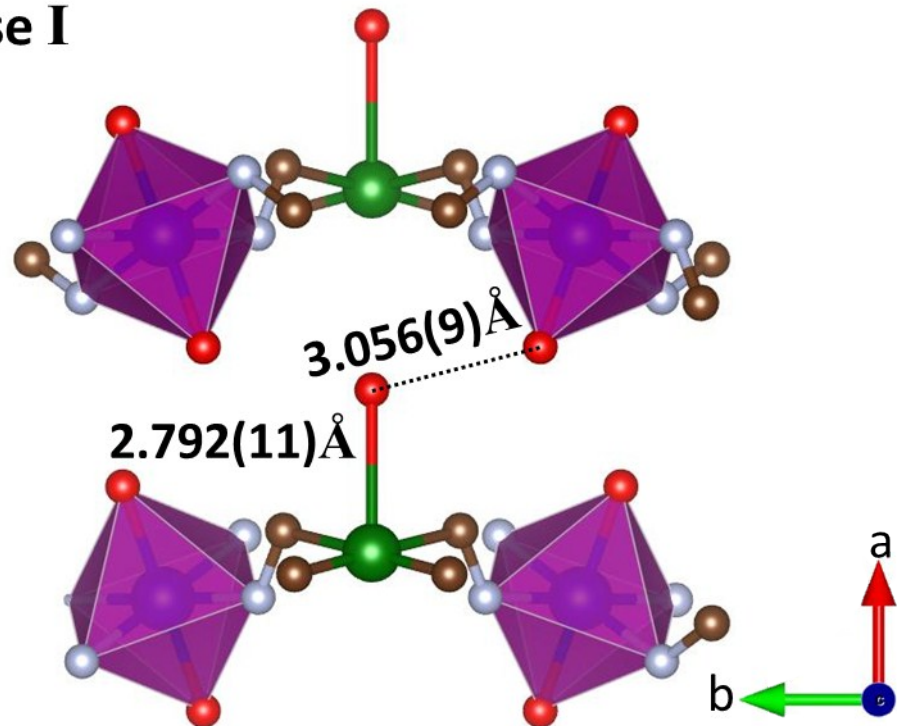


Fig. S3 Thermogravimetric–differential thermal analysis (TG-DTA) for (a) crystal phase I and (b) crystal phase II. The data were collected in air with a scan rate of $5\text{ }^{\circ}\text{C min}^{-1}$. The gradual water molecules weight losses observed below the $150\text{ }^{\circ}\text{C}$ for both phases.

Phase I

a)



Phase II

b)

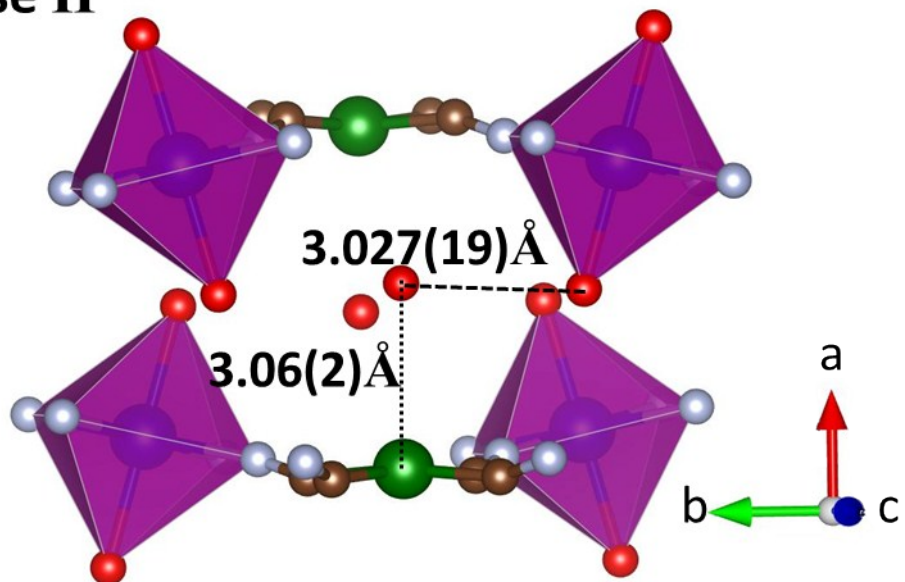


Fig.S4 Distance between oxygen bond and Ni–O coordination bond on a) phase I and b) phase II.

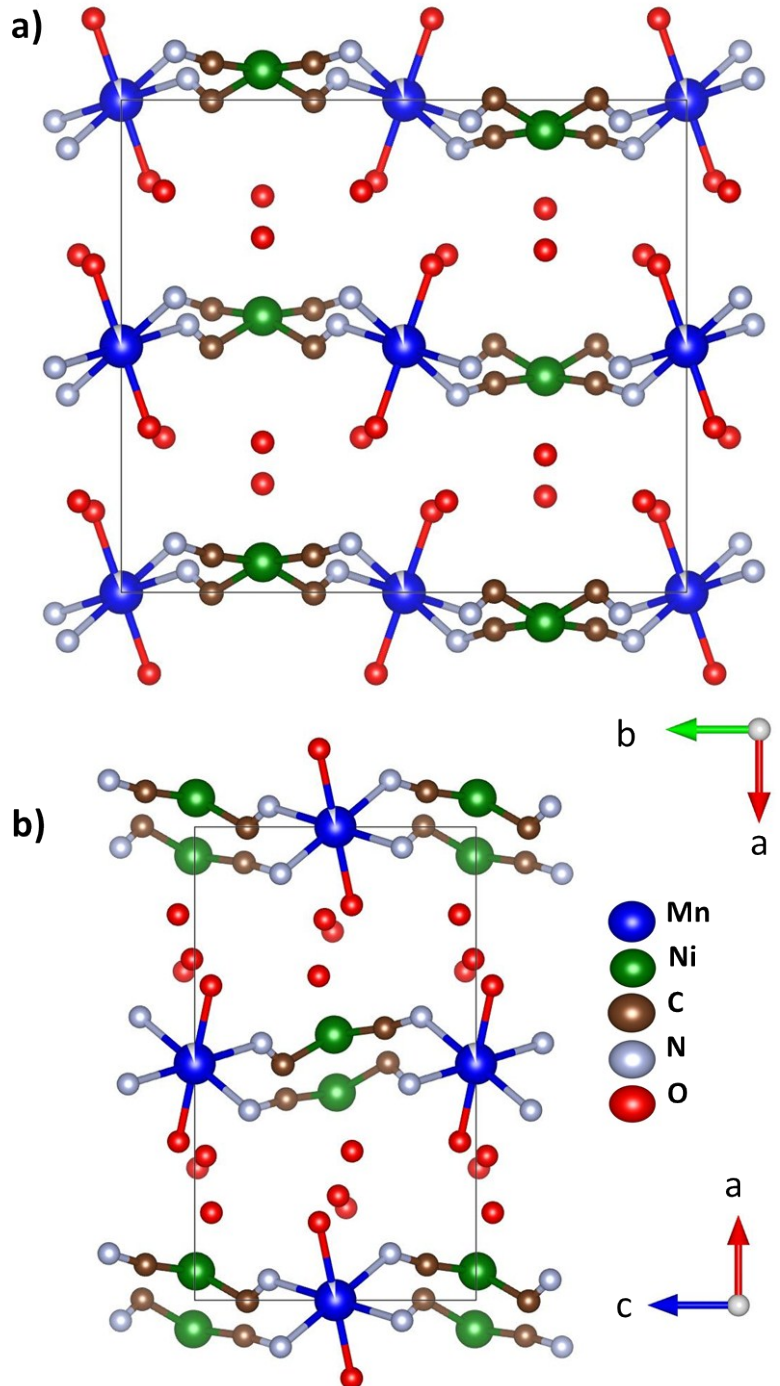


Fig. S5 Crystal structure of re-hydrated sample (phase I) obtained by PXRD.

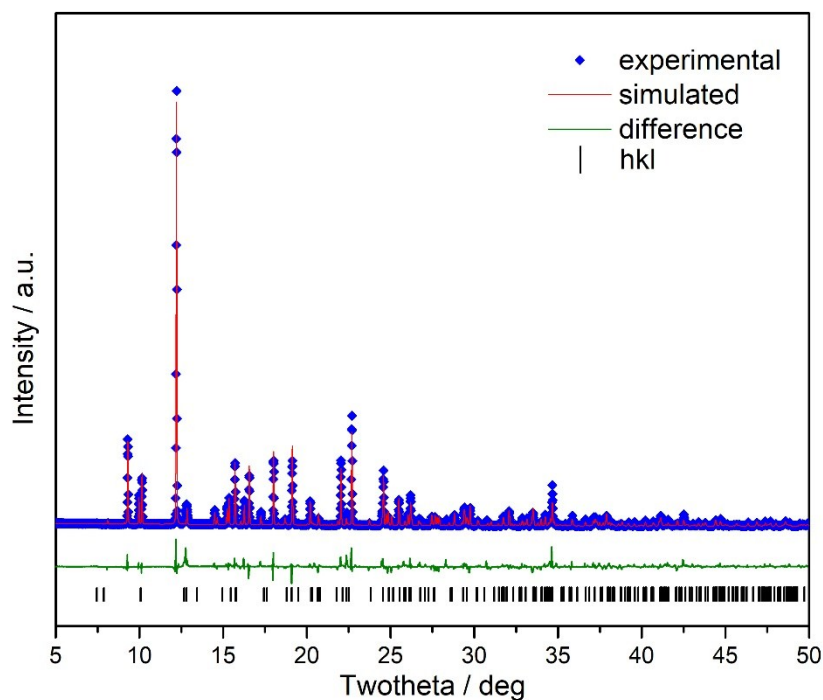


Fig. S6 Rietveld analysis result of the PXRD patterns for rehydrated sample (RH = 100%).

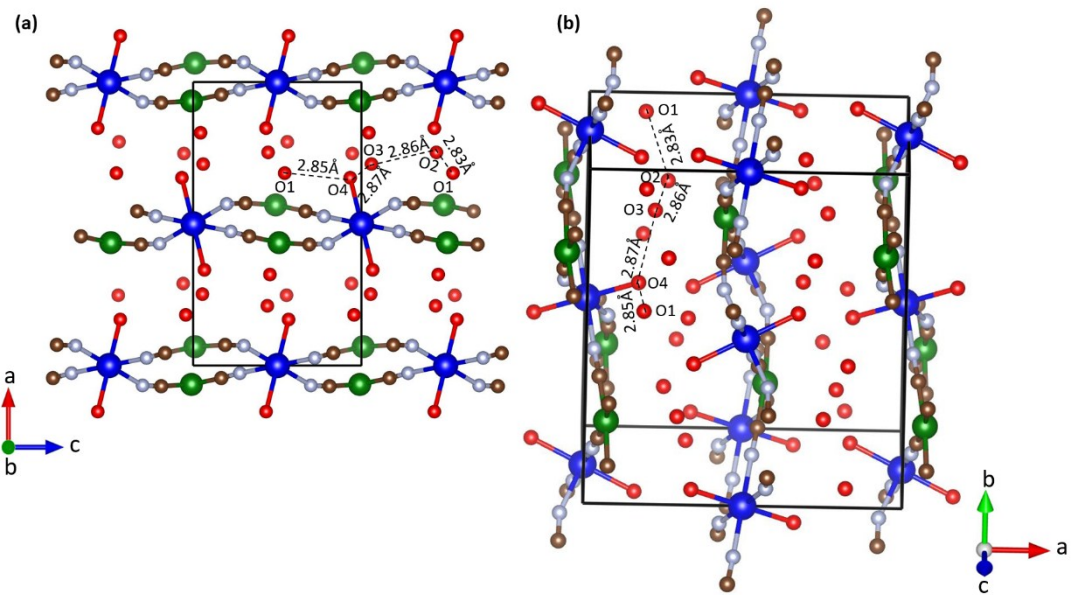


Fig. S7 Hydrogen bonding network and O-O distances in phase I.

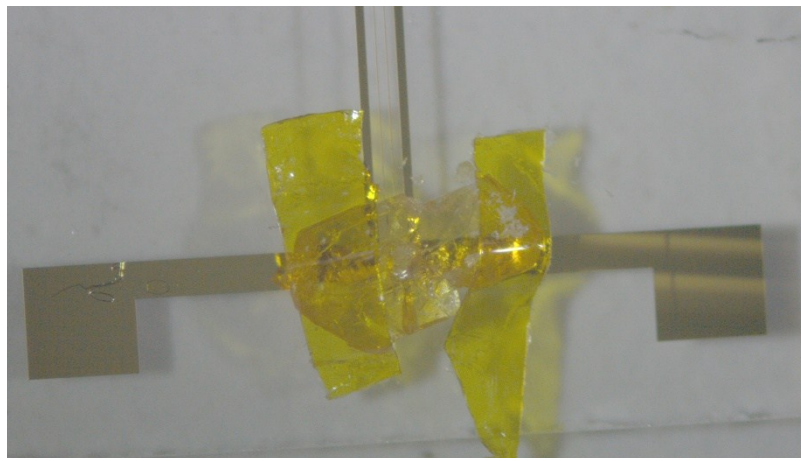


Fig. S8 Photograph of the microelectrodes for the single-crystal impedance measurement. A crystal (1 mm wide x 0.5 mm thick) was contacted with microelectrodes having a 80 nm gap using a Kapton tape.

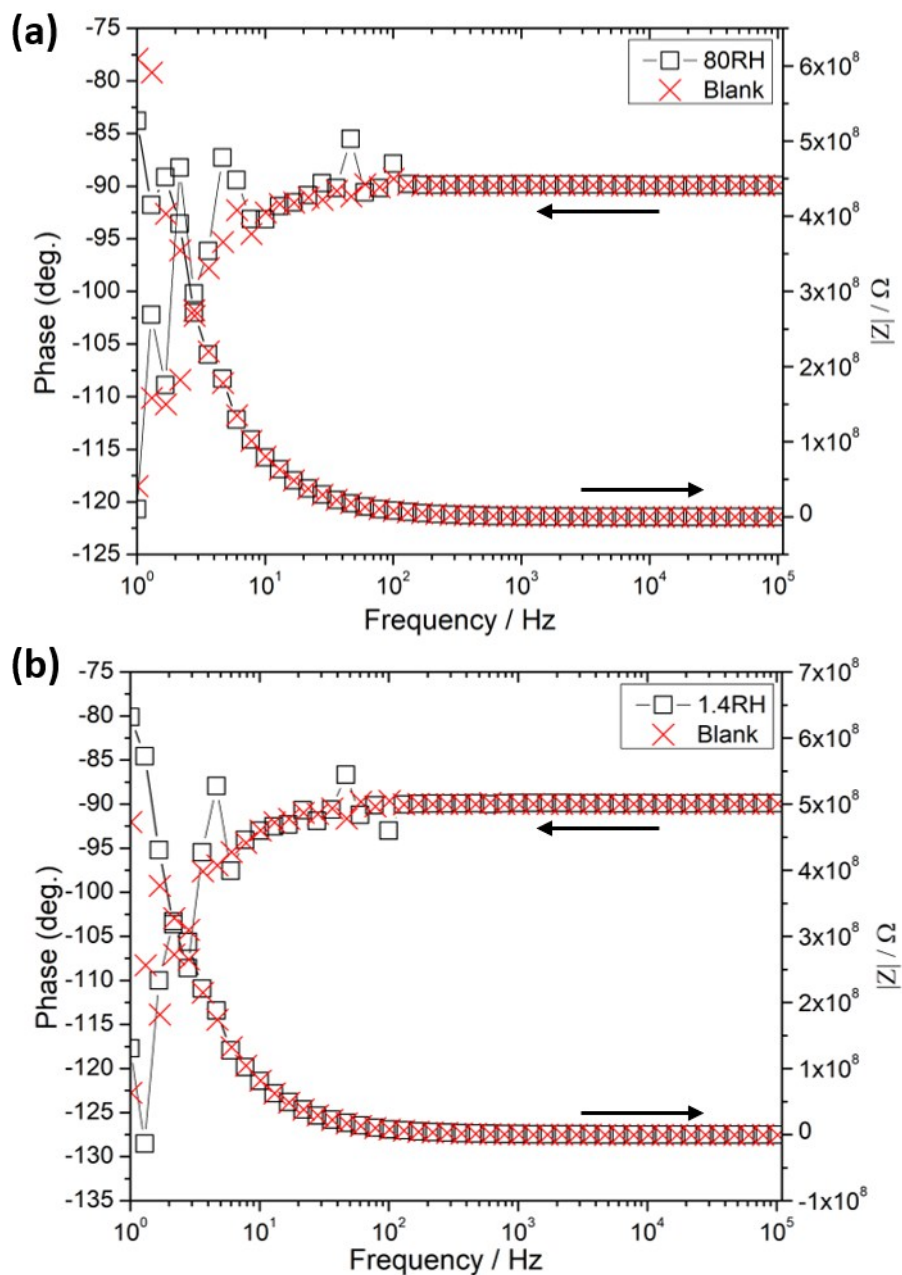


Fig. S9 Bode plots of impedance data for a $\text{Mn}(\text{H}_2\text{O})_2[\text{Ni}(\text{CN})_4]$ single crystal measured at (a) RH = 80% and (b) 1.4%.